

Photocatalytic Preparation of Ag/TiO₂ Films and Their Localized Surface Plasmon Resonance Sensing Properties

Ichiro Tanahashi

Nanomaterials and Microdevices Research Center, Osaka Institute of Technology,
5-16-1 Omiya, Asahi-ku, Osaka 535-8585

Received February 26, 2007; E-mail: tanahashi@chem.oit.ac.jp

Photocatalytic deposition of Ag nanoparticles from AgNO₃ aqueous solution onto TiO₂ films (Ag/TiO₂ films) was carried out by using ultraviolet light irradiation at room temperature. The Ag/TiO₂ films were characterized by XRD, XPS, and SEM. The mean diameter of Ag nanoparticles on the film was estimated to be 113 nm. In the optical absorption spectra of the Ag/TiO₂ film, the localized surface plasmon resonance (LSPR) peak of Ag nanoparticles was observed around 390 nm. A linear relation was clearly observed between the LSPR peak wavelength and the refractive index of the surrounding media, such as alcohols, D-glucose and urea aqueous solutions, in the range of 1.0003–1.4394. The Ag/TiO₂ films were easy to prepare and had a reproducible SPR sensing performance.

Nanomaterials of noble metals, such as gold and silver, have been extensively studied due to their interesting optical and catalytic properties.^{1–5} Especially, in recent years, nanometer-sized gold and silver particles have attracted considerable attention for their applications to sensor devices, such as surface plasmon resonance (SPR) sensors and immunoassays. Conventional SPR sensors with a metal film deposited upon a glass prism are based on the principle that the SPR is highly sensitive to the refraction index of surrounding medium.⁶ The high sensitivity is due to the electric field enhancement at the interface between the metal film and the surrounding medium. In the case of conventional SPR sensors, the index differences are detected via angle changes of a reflected laser beam. The SPR sensors require a glass prism and the optics associated with the detection system for the attenuated total reflection geometry. On the other hand, the localized surface plasmon resonance (LSPR) is observed for gold and silver nanoparticles in the wavelength region of visible light. The optical absorption of the metal nanoparticles at the resonance depends on the refractive index of the surrounding medium of the metal nanoparticles. We can detect a change in the refractive index from changes in the absorption spectrum of the metal nanoparticles. Thus, the SPR sensor with metal nanoparticles do not require a complicated optical system.⁷ Furthermore, the sensor can be small; theoretically, the sensor can be only one nanoparticle. Thus, it reduces the amount of sample required compared to that of conventional SPR sensors.

In order to obtain stable and immobilized metal nanoparticles on the substrates, photocatalytic deposition of silver (Ag) onto titania (TiO₂) films seems to be a useful method. There have been several papers,^{8–11} in which Ag nanoparticles have been deposited on TiO₂ films (Ag/TiO₂ films). The Ag/TiO₂ films have many interesting properties so that there are a variety of applications for the films, such as photochromic displays,⁹ catalysts,¹⁰ and antibacterial materials.¹¹

In a previous study,⁷ we have reported that the photocatalytically prepared Ag/TiO₂ films showed the SPR sensing prop-

erties for the alcohols in the refractive index range of 1.33–1.41. However, direct observation of the Ag nanoparticles of the Ag/TiO₂ films have not been carried out, and the SPR sensing properties of the film for any other solvents have not been clarified. In this paper, the characterization of the Ag/TiO₂ films using XRD, XPS, and SEM and the SPR sensing properties of the films for various kinds of solvents, such as alcohols, D-glucose, urea, NaCl, and H₂SO₄ aqueous solutions, are reported.

Experimental

The preparation process for the Ag/TiO₂ films is outlined in Fig. 1. All compounds were of reagent grade and were used without further purification. A glass slide substrate with a width of 9 mm, a length of 55 mm, and a thickness of 1.0 mm (Matsunami Glass Ind., Ltd., S-1126) was coated with TiO₂ film from anatase sol (Ishihara Sangyo Kaisha, ST-K211) by using a dip-coating technique. The dip and drying procedures were repeated three times, resulting in a TiO₂ film that was about 300 nm in thickness on both sides of the glass slide. The resulting film was soaked in 20 mL of a 0.01 M AgNO₃ aqueous solution in a petri dish about 15 mm away under a 15 W low-pressure mercury lamp (a germicidal lamp) and exposed to UV light irradiation with a power density of 1.0 mW cm^{–2} for 4 h, the deposition of Ag particles onto the TiO₂ film occurred. The resultant Ag/TiO₂ films were washed with distilled water, finally dried in air for more than 12 h. All of the preparation procedures were carried out at room temperature.

X-ray diffraction (XRD) measurements were performed on a RINT 2000 X-ray diffractometer (Rigaku Corporation), using Cu K α radiation working at 40 kV and 40 mA. X-ray photoelectron spectra (XPS) analyses were performed on a Kratos Axis Ultra spectrometer using an Al K α X-ray source. Typical operation conditions: X-ray gun, 15 kV, 10 mA; pressure in the analytical chamber, less than 5.0×10^{-7} Pa. Scanning electron microscopy (SEM) analysis of the Ag/TiO₂ films was carried out using a VE-9800 scanning electron microscope (Keyence Corporation) at an acceleration voltage of 10 kV and a working distance of 7–8 mm.

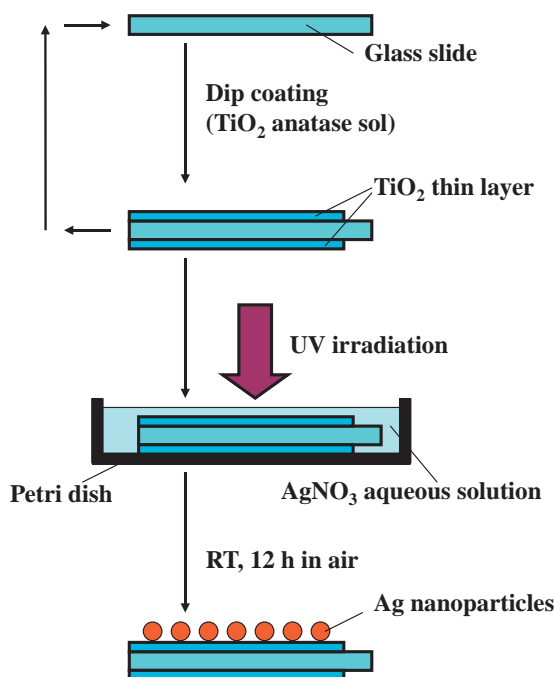


Fig. 1. A schematic illustration for the preparation process of Ag/TiO₂ films.

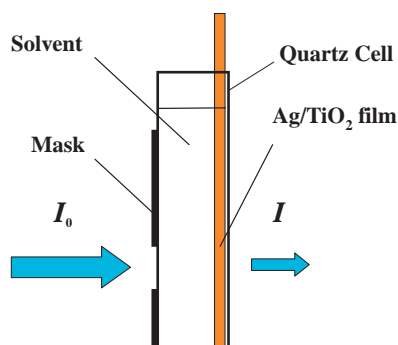


Fig. 2. Typical setup for optical absorption spectrum measurement of the Ag/TiO₂ film.

All absorption spectra were recorded from 200 to 800 nm on an UV-3100PC dual beam spectrophotometer (Shimadzu Corporation) in 10 mm path length quartz liquid cells. Figure 2 shows the typical setup for the absorption spectrum measurement. A matted black-painted stainless steel mask (1 mm in thickness) with a window area of about 28 mm² (6 mm in diameter) was attached to the cell and the Ag/TiO₂ film was positioned in the edge of the cell. The film was sequentially immersed in several different solvents in the cell. Changes in the spectra of the films were sequentially recorded for each immersion. After each measurement, the film was rinsed with methanol and dried at room temperature and used for the next measurement. The alcohols used were as follows: methanol ($n_D^{20} = 1.3292$), ethanol ($n_D^{20} = 1.3605$), 1-propanol ($n_D^{20} = 1.3854$), 1-butanol ($n_D^{20} = 1.3993$), 1-pentanol ($n_D^{20} = 1.4103$), and ethylene glycol ($n_D^{20} = 1.4298$).¹² The n_D^{20} is the refractive index at 20 °C. D-glucose, urea, NaCl, and H₂SO₄ aqueous solutions with various concentrations were also used as the solvents.

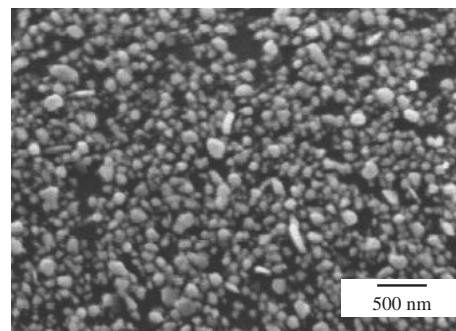


Fig. 3. SEM micrograph of the as-prepared Ag/TiO₂ film.

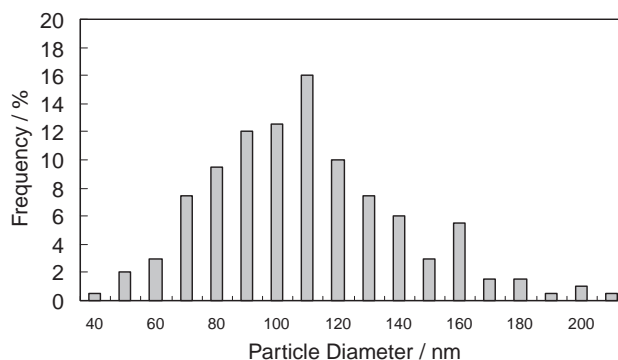


Fig. 4. Particle size distribution of Ag nanoparticles obtained from the analysis of SEM micrograph shown in Fig. 3.

Results and Discussion

Characterization of the Ag/TiO₂ Film. A typical SEM image of the Ag nanoparticles deposited onto the TiO₂ film (as-prepared film) is shown in Fig. 3. In the figure, non-agglomerated Ag nanoparticles were deposited, and they were densely packed. Polygonal-shaped nanoparticles with diameters of 40–200 nm were observed. The deposited Ag nanoparticles were not washed off by distilled water and organic solvents, such as methanol and ethanol. Thus, the nanoparticles are immobilized on the TiO₂ film by the photocatalytic reaction. Figure 4 shows the particle size distribution obtained from the analysis of the SEM micrograph of the film shown in Fig. 3. A part of the micrograph field including 200 particles was randomly selected to analyze the size distribution. The average diameter of the particles was 113 nm with a standard deviation of 32 nm. The size of the nanoparticles was larger than that in the literature.⁸ The color of the film was brownish-gray not transparent yellow, suggesting that the size distribution of the Ag particles is large.

XPS experiments were performed to elucidate the chemical state of Ag nanoparticles on the TiO₂ film. Figure 5 shows the Ag 3d electron spectrum of the Ag/TiO₂ film shown in Fig. 3. To compensate for sample charging, binding energies were referenced to that of the carbon 1s peak at 285.0 (±0.21) eV. In the spectrum, there are two peaks (the spin doublet of Ag 3d) centered at 368.0 and 374.1 eV (corresponding to Ag 3d_{5/2} and Ag 3d_{3/2}, respectively). The splitting of the 3d doublet was 6.07 eV. These values correspond to metallic Ag.⁸ Furthermore, no peak corresponding to Ag₂O (367.8 eV) or

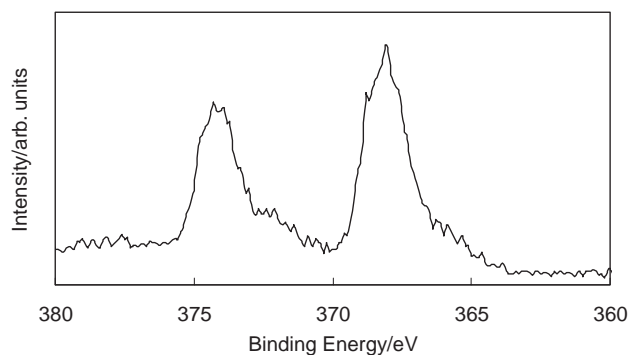


Fig. 5. Ag 3d electron spectrum of the Ag/TiO₂ film.

AgO (367.4 eV) was observed in XPS spectra of the Ag/TiO₂ film. The Ag species deposited on TiO₂ film were all metallic Ag, not Ag₂O or AgO. In accordance with these results, in the XRD pattern of the Ag/TiO₂ film, the peaks at $2\theta = 38.1^\circ$ and at $2\theta = 44.3^\circ$ were observed and respectively, assigned to the (111) and (200) reflection lines of cubic Ag. In this XPS experiments, the O 1s peak and Ti 2p peak were not clearly observed. This is probably due to the low amount of TiO₂ in Ag/TiO₂ film and the TiO₂ film was densely covered with Ag nanoparticles. Peaks associated with TiO₂ were also not observed in the XRD pattern. However, in the XRD pattern of the TiO₂ powder prepared from drying sol (ST-K211), which was used for preparing the TiO₂ film, at 70 °C clearly exhibited peaks at $2\theta = 25.3, 37.8, 48.0,$ and 53.9° , which were assigned to the (101), (004), (200), and (211) reflection lines of the anatase form of TiO₂, respectively. From these results, nanosized metal Ag nanoparticles were successfully deposited on the anatase form of TiO₂ film by using a photocatalytic process.

SPR Sensing Properties of the Ag/TiO₂ Film. Absorption spectrum of the Ag/TiO₂ film in air and that of the film immersed in six different alcohols i.e., methanol, ethanol, 1-propanol, 1-butanol, 1-pentanol, and ethylene glycol, aqueous solutions of ethylene glycol (20, 40, 60, and 80 wt %), and distilled water were measured. It has already been reported that the peak absorbance of an immersed film in the five alcohols (methanol, ethanol, 1-propanol, 1-butanol, and 1-pentanol) increased and the absorption peak wavelength shifted to longer wavelengths with an increase in the refractive index, n , of the alcohols.⁷ A linear relationship was observed between the peak wavelength and the n of the alcohols in the range of 1.33–1.41.⁷

Figure 6a shows the absorption spectra of the Ag/TiO₂ film and the film sequentially immersed in distilled water (indicated as 0 wt % in the figure), aqueous solutions of ethylene glycol (20, 40, 60, and 80 wt %), and ethylene glycol (100 wt %). In the figure, the film in air shows an absorption peak at 387.5 nm, due to the LSPR absorption of the Ag nanoparticles. The broad absorption band of the film suggests that the size distribution of Ag nanoparticles is large. It is known that the absorbance and the peak wavelength of the LSPR absorption of metal nanoparticles are influenced by the size and shape of the metal particles themselves, the density of the particles, and the kinds of substrates, on which the metal nanoparticles are deposited. In Fig. 6a, the broad absorption band at a longer

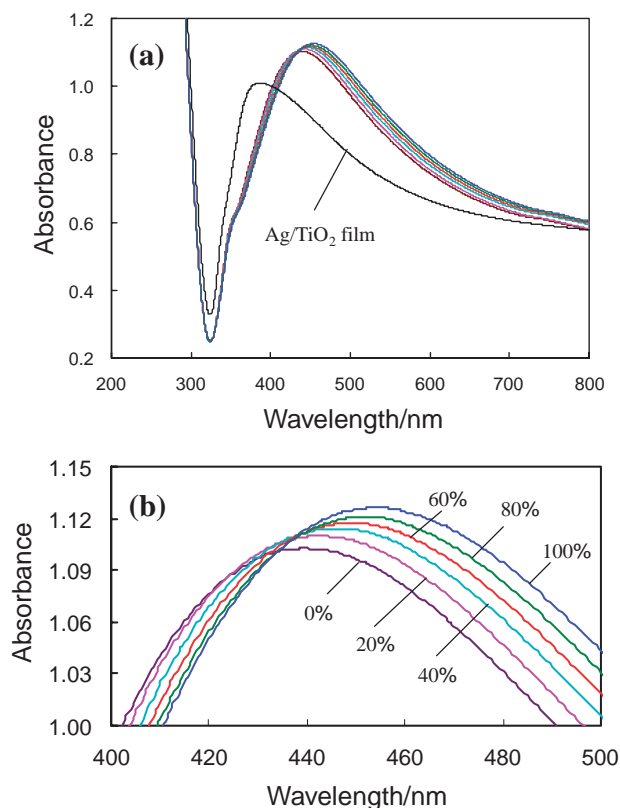


Fig. 6. Optical absorption spectra of the Ag/TiO₂ film and the film immersed in the alcohols with different refractive index: (a) in the range of 200–800 nm and (b) near the LSPR peak wavelength of the spectra for the immersed film.

wavelength than of the LSPR peak is probably due to the larger size Ag nanoparticles and the light scattering of the film. The absorption spectra of the magnified scale for the immersed film near the LSPR peak are shown in Fig. 6b. It is known that the absorbance maximum increases with the n of the surrounding medium.¹³ In Fig. 6b, in accordance with this expectation, the peak absorbance of the immersed film increased from 1.010 (in air) to 1.126. In the figure, the absorption peak wavelength clearly shifted to longer wavelengths from 387.5 (in air) to 454.5 nm with an increase in the n of the surrounding alcohols. Figures 7a and 7b show the LSPR peak absorbance (a) and the LSPR peak wavelength (b) of the Ag/TiO₂ film as a function of the n of the surrounding alcohols, respectively. Over the range of n studied here (1.0003–1.4298), a linear relationship ($R = 0.999$, R : correlation coefficient) with a slope of 0.27 absorbance unit (AU)/refractive index unit (RIU) was observed. A linear relationship ($R = 0.999$) between the LSPR peak wavelength and n with a sensitivity of 156 nm/RIU was also observed. The spectral change in the LSPR band was reproducible when the film was immersed into the alcohols used here. Thus, the Ag/TiO₂ film can function as a SPR sensor repeatedly, only if they are rinsed with distilled water, methanol, and ethanol, and then dried at room temperature.

Table 1 gives the peak position of the LSPR band of the Ag/TiO₂ film with the variation in solvent refractive indices

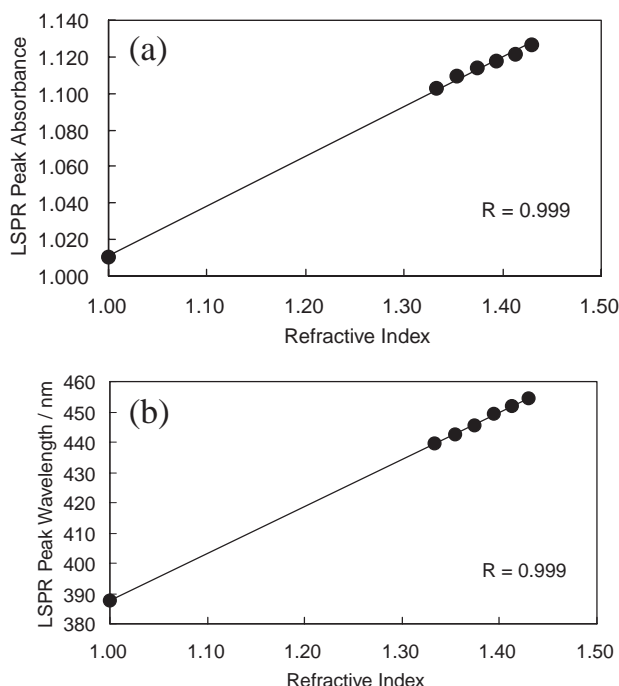


Fig. 7. Plot of the LSPR peak absorbance (a) and LSPR peak wavelength (b) as a function of the refractive index of the alcohols.

Table 1. Peak Positions of the LSPR Absorbance Wavelength and the Refractive Indices of Solvents

Solvent	Refractive index (n_D^{20})	Peak position/nm
Air	1.0003	387.5
Methanol	1.3292	438.5
Ethanol	1.3605	445.0
1-Propanol	1.3854	446.5
1-Butanol	1.3993	450.5
1-Pentanol	1.4103	451.0
Ethylene glycol (EG)	1.4298	454.5
Water	1.3330	439.5
20 wt % EG	1.3540	442.5
40 wt % EG	1.3745	445.5
60 wt % EG	1.3943	449.5
80 wt % EG	1.4130	452.0

at 20 °C. When the film was sequentially immersed in the solvents in Table 1, a linear relation ($R = 0.999$) was also clearly observed between the peak wavelength and the n . A linear fit to the plot of the peak wavelength as a function of n gave a sensitivity of 156 nm/RIU. This value was two times larger than that of Au nanoparticles in the literature.¹⁴ It seems that the sensitivity of the SPR sensor with Ag nanoparticles with 113 nm is better than that of the sensor with Au nanoparticles with 13 nm in diameter.¹⁴ Further investigations are necessary to clarify the difference in the sensitivity of the SPR sensing properties between Ag and Au nanoparticles.

According to Mie theory,^{13,15–17} the LSPR peak position, λ , is related to n of the surrounding medium by the following equation:

$$\lambda^2 = \lambda_p^2(\epsilon^\infty + 2n^2), \quad (1)$$

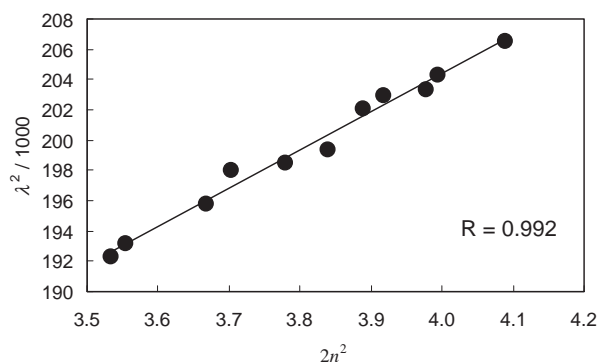


Fig. 8. The square of the LSPR peak absorbance wavelength as a function of twice the square of the refractive indices of the alcohols.

where λ_p is the bulk metal plasmon wavelength, ϵ^∞ the high-frequency dielectric constant due to interband and core transitions. λ_p is expressed by the following equation:

$$\lambda_p = 2\pi c / \omega_p, \quad (2)$$

where c is the speed of light in a vacuum and ω_p the metal's bulk plasma frequency given by

$$\omega_p = \left(\frac{Ne^2}{m\epsilon_0} \right)^{1/2}, \quad (3)$$

where N is the free electron concentration in metal, m the electron mass (9.109×10^{-31} kg), e elementary electric charge (1.602×10^{-19} C), and ϵ_0 dielectric constant in a vacuum (8.854×10^{-12} F m⁻¹). The n of the medium is directly related to its dielectric constant (ϵ_m), i.e., $n = \sqrt{\epsilon_m}$. In the case of silver, it is reported that the value of N is 5.8×10^{28} m⁻³. Using these values, ω_p of silver was calculated to be 1.36×10^{16} s⁻¹ and λ_p 139 nm. From Eq. 1, a plot of λ^2 as a function of $2n^2$ should be linear. Figure 8 shows the relation between λ^2 of the LSPR of the Ag//TiO₂ film and $2n^2$ of the surrounding alcohols given in Table 1. In the figure, over the range of n of the solvents studied here, a linear relation ($R = 0.992$) was observed. According to Mie theory, the linear relation between λ^2 and $2n^2$ is indicative of the fact that the alcohol refractive index influences the LSPR peak wavelength. From Fig. 8, λ_p was calculated to be 159 nm, which is close to the value (139 nm) calculated from the Eqs. 2 and 3. It was concluded that the Ag//TiO₂ film has a SPR sensing ability for solvents in the n range of 1.3292–1.4298.

Figure 9 shows the LSPR peak wavelength of the Ag/TiO₂ film and the film immersed in distilled water and D-glucose aqueous solutions with different concentrations (10, 20, 30, 40, 50, and 60 wt %). The values of n_D^{20} for the refractive index of 10, 20, 30, 40, 50, and 60 wt % D-glucose aqueous solution are 1.3477, 1.3635, 1.3805, 1.3986, 1.4181, and 1.4394, respectively.¹² Similar to the result shown in Fig. 7b, in Fig. 9, the LSPR absorption peak wavelength clearly shifted to longer wavelengths from 390.5 (in air) to 444.5 nm with an increase in the n of the surrounding D-glucose aqueous solution. Over the n range of (1.0003–1.4394), a linear relationship ($R = 0.999$) between the LSPR peak wavelength of the film and the n of the D-glucose aqueous solutions with a sensitivity of 122 nm/RIU. Beside the D-glucose aqueous solu-

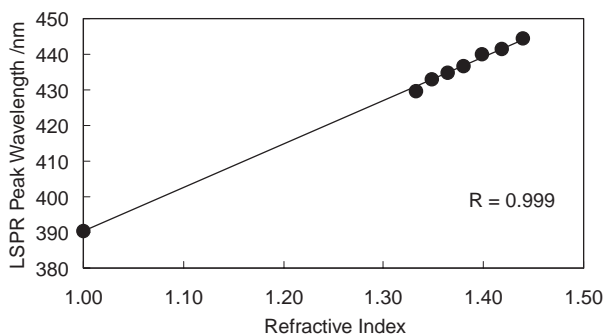


Fig. 9. Plot of the LSPR peak wavelength as a function of the refractive index of the D-glucose aqueous solutions.

tions, when the film was immersed in urea aqueous solutions with different concentrations (10, 20, 30, and 40 wt %), a linear relationship ($R = 0.998$) was also observed between the LSPR absorption peak wavelength and the n of the surrounding urea aqueous solutions. The n_D^{20} of the urea aqueous solutions used here is in the range of 1.3476–1.3947.¹² However, when the film was immersed into 5 wt % NaCl and 1 wt % H₂SO₄ aqueous solutions, the Ag nanoparticles peeled off from the substrate after a few minutes. The Ag/TiO₂ film did not show a SPR sensing ability for NaCl and H₂SO₄ aqueous solutions. The Ag nanoparticles probably react with chloride ions and sulfate ions.

Summary

In this study, the preparation and the characterization of the Ag/TiO₂ films and their SPR sensing properties were investigated. Ag nanoparticles were successfully deposited onto the TiO₂ film by photocatalytic reaction at room temperature. The deposited Ag nanoparticles were immobilized onto the TiO₂ film, and the average diameter of the particles was 113 nm with a standard deviation of 32 nm. The color of the film was brownish-gray not transparent yellow, suggesting that the size distribution of the Ag particles is large. From the XPS and XRD measurements, the Ag species deposited on TiO₂ film were all metallic Ag, and not Ag₂O or AgO.

The Ag/TiO₂ film showed an absorption peak around 390 nm, due to the LSPR absorption of the Ag nanoparticles. When the film was sequentially immersed in different solvents, such as alcohols, D-glucose and urea aqueous solutions, in the refractive index range of 1.0003–1.4394, a linear relation was clearly observed between the SPR peak wavelength and the refractive index of the solvents. However, the film did not show a SPR sensing ability for NaCl and H₂SO₄ aqueous solutions due to the reaction between Ag nanoparticles and chloride ions and sulfate ions. On the other hand, when the film was im-

mersed in different alcohols, a linear fit to the plot of the peak wavelength as a function of the refractive index gave a sensitivity of 156 nm/RIU (refractive index unit). A linear relationship ($R = 0.992$) was also observed between the square of the observed peak position, λ^2 , of the LSPR of the Ag//TiO₂ film and the twice of the square of the refractive index, $2n^2$, of the surrounding alcohols with a refractive index in the range of 1.3292–1.4298. According to Mie theory, the linear relation between λ^2 and $2n^2$ is indicative of the fact that the solvent refractive index influences the LSPR peak wavelength. The absorption spectra changes were reproducible for all the solvents studied here. It was concluded that the Ag//TiO₂ film showed a SPR sensing ability for alcohols, D-glucose and urea aqueous solutions over a wide range of n .

The author is thankful to Mr. Fumitake Yamazaki for his experimental help and Mr. Yoshihisa Kinoshita for the SEM measurements.

References

- 1 U. Kreibig, C. v. Fragstein, *Z. Phys.* **1969**, 224, 307.
- 2 D. Ricard, P. Roussignal, C. Flytzanis, *Opt. Lett.* **1985**, 10, 511.
- 3 I. Tanahashi, Y. Manabe, T. Tohda, S. Sasaki, A. Nakamura, *J. Appl. Phys.* **1996**, 79, 1244.
- 4 H. Inouye, K. Tanaka, I. Tanahashi, K. Hirao, *Phys. Rev. B* **1998**, 57, 11334.
- 5 M. Haruta, N. Yamada, T. Kobayashi, S. Iijima, *J. Catal.* **1989**, 115, 301.
- 6 E. Kretschmann, *Z. Phys.* **1971**, 241, 313.
- 7 I. Tanahashi, F. Yamazaki, K. Hamada, *Chem. Lett.* **2006**, 35, 454.
- 8 E. Stathatos, P. Lianos, P. Falaras, A. Siokou, *Langmuir* **2000**, 16, 2398.
- 9 Y. Ohko, T. Tatsuma, T. Fujii, K. Naoi, C. Niwa, Y. Kubota, A. Fujishima, *Nat. Mater.* **2003**, 2, 29.
- 10 Y. Chen, C. Wang, H. Liu, J. Qiu, X. Bao, *Chem. Commun.* **2005**, 5298.
- 11 J. Keleher, J. Bashant, N. Heldt, L. Johnson, Y. Li, *World J. Microbiol. Biotechnol.* **2002**, 18, 133.
- 12 *Kagakubinran Kisohen Part 2*, ed. by Chemical Society of Japan, Tokyo, Maruzen, **1984**.
- 13 A. C. Templeton, J. J. Pietron, R. W. Murray, P. Mulvaney, *J. Phys. Chem. B* **2000**, 104, 564.
- 14 N. Nath, A. Chilkoti, *Anal. Chem.* **2002**, 74, 504.
- 15 G. Mie, *Ann. Phys.* **1908**, 25, 377.
- 16 A. Henglein, *J. Phys. Chem.* **1993**, 97, 5457.
- 17 S. K. Ghosh, S. Nath, S. Kundu, K. Esumi, T. Pal, *J. Phys. Chem. B* **2004**, 108, 13963.